Eur. Phys. J. C (2017) 77:694
DOI 10.1140/epjc/s10052-017-5282-y

THE EUROPEAN PHYSICAL JOURNAL C

Regular Article - Theoretical Physics

Explaining the R_K and R_{K^*} anomalies

Diptimoy Ghosh[a]

Department of Particle Physics and Astrophysics, Weizmann Institute of Science, 76100 Rehovot, Israel

Received: 20 August 2017 / Accepted: 3 October 2017 / Published online: 20 October 2017

Abstract Recent LHCb results on R_{K^*}, the ratio of the branching fractions of $B \to K^*\mu^+\mu^-$ to that of $B \to K^*e^+e^-$, for the dilepton invariant mass bins $q^2 \equiv m^2_{\ell\ell} =$ [0.045–1.1] GeV^2 and [1.1–6] GeV^2 show approximately 2.5σ deviations from the corresponding Standard Model prediction in each of the bins. This, when combined with the measurement of R_K ($q^2 = [1-6]\,\mathrm{GeV}^2$), a similar ratio for the decay to a pseudo-scalar meson, highly suggests lepton non-universal new physics in semi-leptonic B meson decays. In this work, we perform a model independent analysis of these potential new physics signals and identify the operators that do the best job in satisfying all these measurements. We show that heavy new physics, giving rise to q^2 independent local 4-Fermi operators of scalar, pseudo-scalar, vector or axial-vector type, is unable to explain all the three measurements simultaneously, in particular R_{K^*} in the bin [0.045–1.1], within their experimental 1σ regions. We point out the possibility to explain R_{K^*} in the low bin by an additional light ($\lesssim$ 20 MeV) vector boson with appropriate coupling strengths to $(\bar{b}\,s)$ and $(\bar{e}\,e)$.

1 Introduction

The LHCb collaboration has recently reported hints of new physics (NP) in lepton flavor non-universal observables R_K and R_{K^*},

$$R_{K^{(*)}} = \frac{\mathcal{B}\left(B \to K^{(*)}\mu^+\mu^-\right)}{\mathcal{B}\left(B \to K^{(*)}e^+e^-\right)}\,. \tag{1.1}$$

While the result for R_K was presented only in the dilepton invariant mass squared, $q^2 \in$ [1–6] GeV^2, R_{K^*} has been measured in two bins, [0.045–1.1] GeV^2 and [1.1–6] GeV^2. The experimental results are summarised in Table 1.

While the deviations from the Standard Model (SM) in the individual ratios are only at the level of 2.2σ–2.5σ, the combined deviation (the exact number depends on how one combines the 3 results) is large enough to look for NP explanations.[1] For recent studies, see [4,13–19].

At the quark level, the decays $B \to K^{(*)}\mu^+\mu^-$ proceed via $b \to s$ flavor changing neutral current (FCNC) transitions. These decays are particularly interesting because they are highly suppressed in the SM and many extensions of the SM are capable of producing measurable effects beyond the SM. In particular, the three body decay $B \to K^*\mu^+\mu^-$ offers a large number of observables in the angular distributions of the final state particles, hence providing a lot of opportunities to test the SM; see for example [20–49] and the references therein for related studies.

The individual branching ratios $\mathcal{B}\left(B \to K^{(*)}\mu^+\mu^-\right)$ and $\mathcal{B}\left(B \to K^{(*)}e^+e^-\right)$ are predicted with comparatively larger hadronic uncertainties in the SM. However, their ratio is a theoretically clean observable and predicted to be close to unity in the SM. This is in contrast to some of the angular observables (for example, P_5') where considerable debate exists surrounding the issue of theoretical uncertainty due to (unknown) power corrections to the factorization framework and non-local charm loops; see for example [29,50–57]. Hence the observed deviation from the SM might be (at least partly) resolved once these corrections are better understood.

Therefore, in this work we will only consider the theoretically clean observables $R_{K^{(*)}}$ listed in Table 1. Additionally, we also consider the branching ratios of the fully leptonic decays $B_s \to \mu^+\mu^-$ and $B_s \to e^+e^-$, as they are very well predicted in the SM.

The paper is organized as follows. In the next section, we show the complete set of operators at the dimension 6 level for $b \to s\,\ell\,\ell$ transition. In Sect. 3 we discuss in detail how these various operators perform in explaining the $R_{K^{(*)}}$ anomalies, and point out the possibility of explaining R_{K^*} in

[1] Similar anomalies have also been observed in the charged current decays ($B \to D^{(*)}\tau\nu/B \to D^{(*)}\ell\nu$) that call for lepton non-universal new physics. See [11,12] for some recent studies.

[a] e-mail: diptimoy.ghosh@weizmann.ac.il

Table 1 The observables used in our analysis along with their SM predictions and experimental measurements. Note that the QED corrections to R_K and R_{K^*} in the bin $q^2 = [1, 6]\,\mathrm{GeV}^2$ were first calculated in [2]. However, no such calculation exists for R_{K^*} in the bin $q^2 = [0.045, 1.1]\,\mathrm{GeV}^2$

Observable	SM prediction		Measurement	
$R_K : q^2 = [1, 6]\,\mathrm{GeV}^2$	1.00 ± 0.01	[1,2]	$0.745^{+0.090}_{-0.074} \pm 0.036$	[3]
$R_{K^*}^{\rm low} : q^2 = [0.045, 1.1]\,\mathrm{GeV}^2$	0.92 ± 0.02	[4]	$0.660^{+0.110}_{-0.070} \pm 0.024$	[5]
$R_{K^*}^{\rm central} : q^2 = [1.1, 6]\,\mathrm{GeV}^2$	1.00 ± 0.01	[1,2]	$0.685^{+0.113}_{-0.069} \pm 0.047$	[5]
$\mathcal{B}(B_s \to \mu^+\mu^-)$	$(3.57 \pm 0.16) \times 10^{-9}$	[6,7]	$(3.00 \pm 0.5) \times 10^{-9}$	[7–9]
$\mathcal{B}(B_s \to e^+e^-)$	$(8.35 \pm 0.39) \times 10^{-14}$	[6,7]	$< 2.8 \times 10^{-7}$	[10]

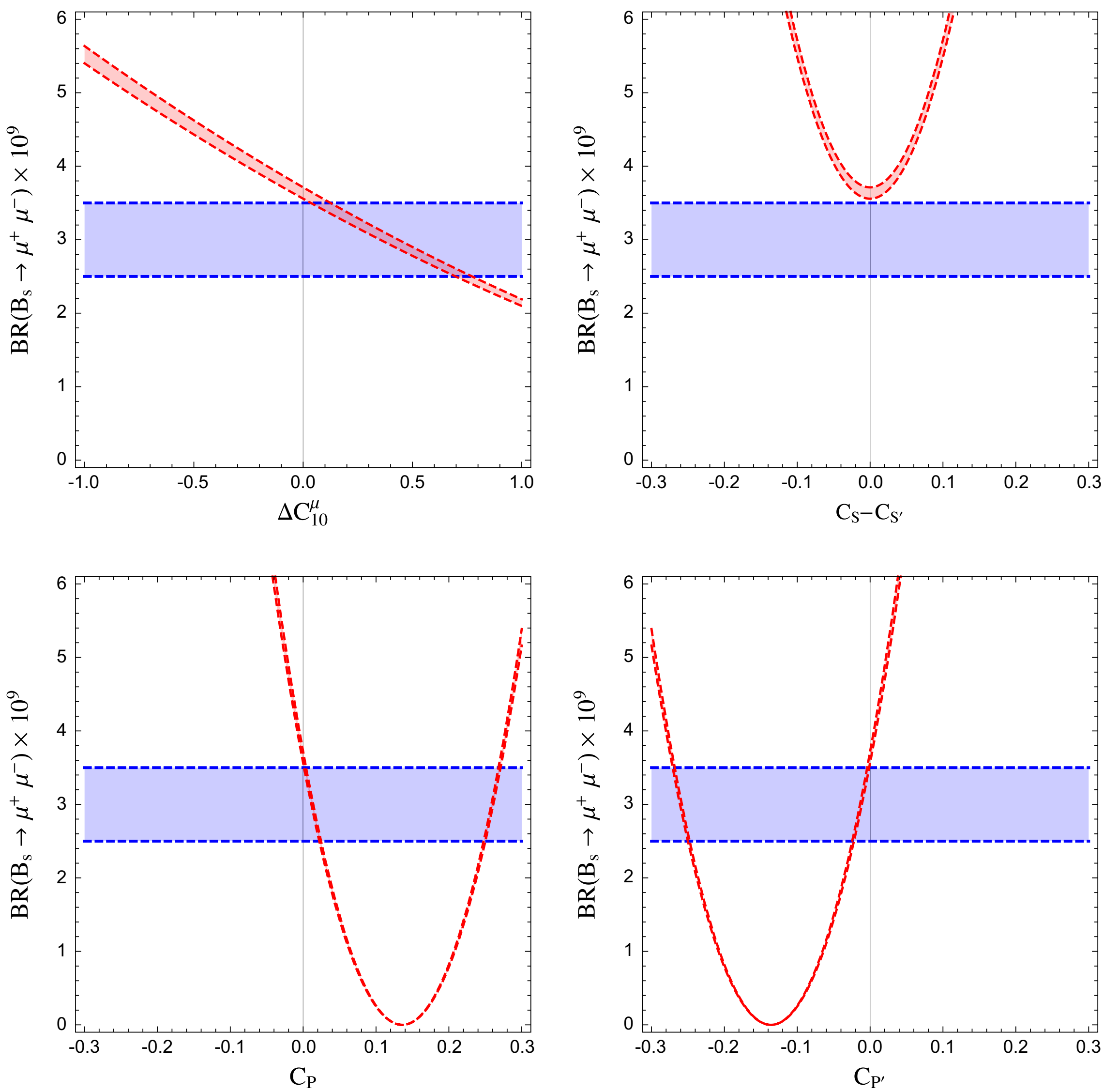

Fig. 1 Variation of the branching ratio of $B_s \to \mu^+\mu^-$ with ΔC_{10}^{μ} and the (pseudo) scalar operaors

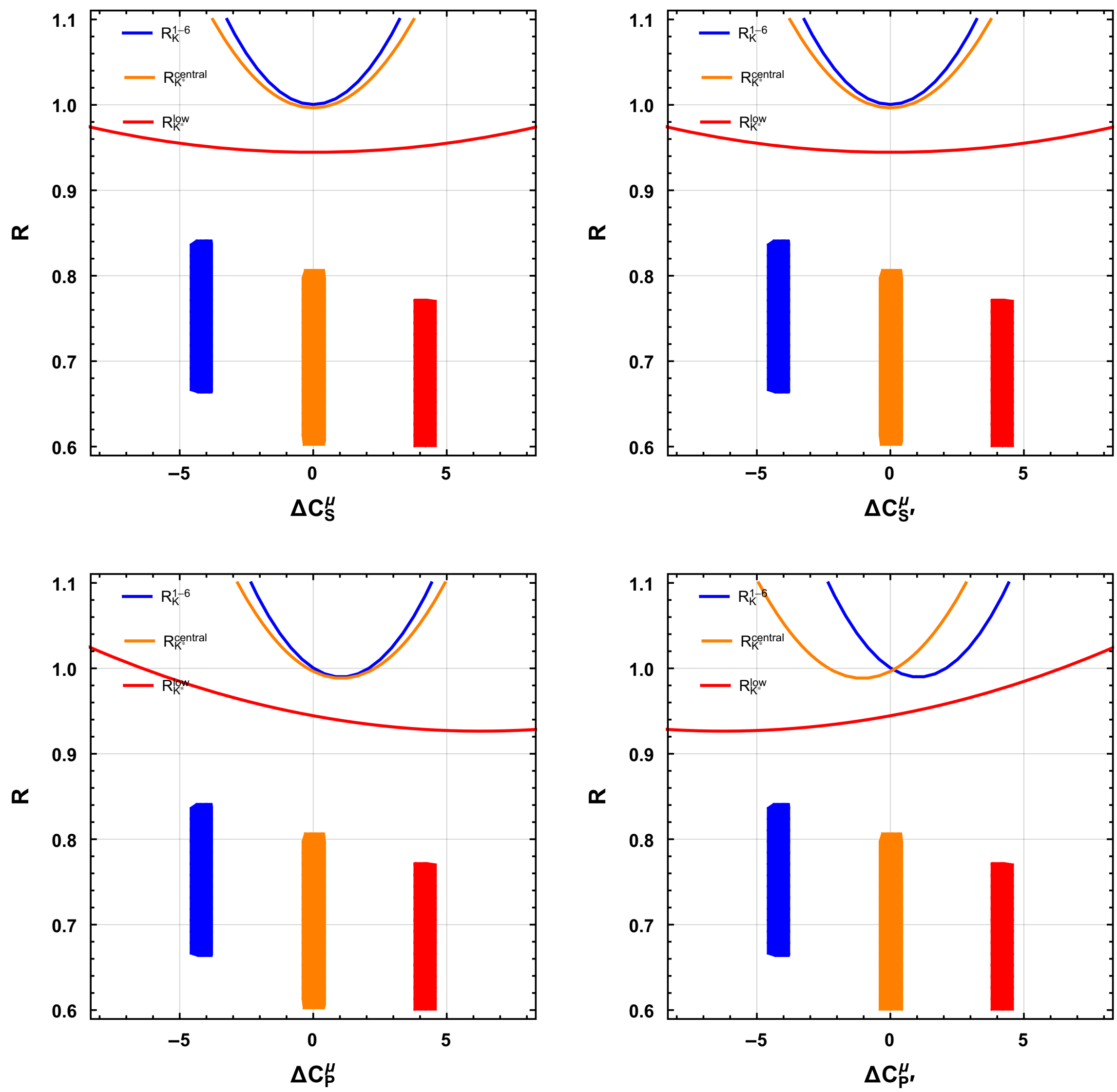

Fig. 2 Variations of R_K, $R_{K^*}^{\rm low}$ and $R_{K^*}^{\rm central}$ with the Wilson coefficients of the various scalar and pseudo-scalar operators involving muons. The vertical bands correspond to the experimental 1σ allowed regions (and independent of ΔC)

the low q^2 bin by a very light gauge boson. We close in Sect. 4 with a brief summary.

2 $b \to s$ effective Hamiltonian

The effective Hamiltonian for $b \to s$ transitions in the Standard Model is given by

$$\mathcal{H}_{\rm eff} = -\frac{4G_F}{\sqrt{2}}\left(\lambda_t^{(s)}\mathcal{H}_{\rm eff}^{(t)} + \lambda_u^{(s)}\mathcal{H}_{\rm eff}^{(u)}\right) + {\rm h.c.}\,, \tag{2.1}$$

with the CKM matrix combinations $\lambda_q^{(s)} = V_{qb}V_{qs}^*$, and

$$\mathcal{H}_{\rm eff}^{(t)} = C_1\mathcal{O}_1^c + C_2\mathcal{O}_2^c + \sum_{i=3}^{6} C_i\mathcal{O}_i + \sum_{i=7}^{10} C_i\mathcal{O}_i\,,$$
$$\mathcal{H}_{\rm eff}^{(u)} = C_1(\mathcal{O}_1^c - \mathcal{O}_1^u) + C_2(\mathcal{O}_2^c - \mathcal{O}_2^u). \tag{2.2}$$

$C_i \equiv C_i(\mu)$ and $\mathcal{O}_i \equiv \mathcal{O}_i(\mu)$ are the Wilson coefficients and the local effective operators, respectively. In order to study the most general NP in $b \to s\, l^+l^-$ transitions, we augment $\mathcal{H}_{\rm eff}^{(t)}$ by

$$\mathcal{H}_{\rm eff}^{(t),\,{\rm New}} = \sum_{i=7,9,10} C_{i'}\mathcal{O}_{i'} + \sum_{i=S,P}(C_i\mathcal{O}_i + C_{i'}\mathcal{O}_{i'}) + \sum_{i=T,T5} C_i\mathcal{O}_i\,, \tag{2.3}$$

where the definitions of the local operators are given by

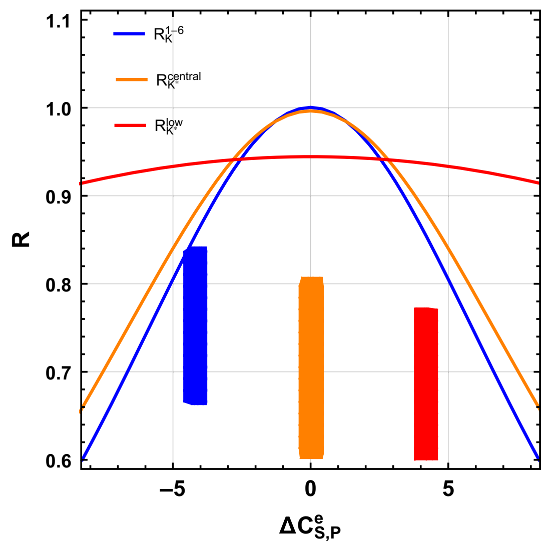

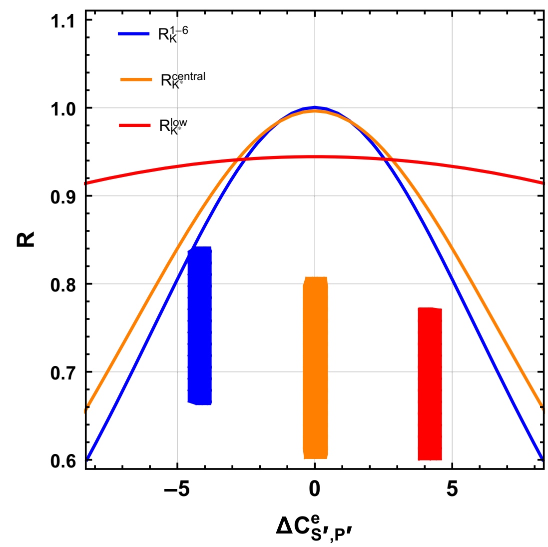

Fig. 3 Variations of R_K, $R_{K^*}^{\text{low}}$ and $R_{K^*}^{\text{central}}$ with the Wilson coefficients of the various scalar and pseudo-scalar operators involving electrons. The variations with the different Wilson coefficients are the same in this case because the decay rate for $B \to K^{(*)}e^+e^-$ dominantly depends on their modulus squared with the same coefficients. The linear interference terms, which have different coefficients for the different operators, are negligible because they are proportional to the electron mass [23]. The vertical bands correspond to the experimental 1σ allowed regions (and independent of ΔC)

$$\begin{aligned}
\mathcal{O}_7 &= \frac{e}{16\pi^2} m_b(\bar{s}\sigma_{\mu\nu}P_R b)F^{\mu\nu},\\
\mathcal{O}_9 &= \frac{\alpha_{\text{em}}}{4\pi}(\bar{s}\gamma_\mu P_L b)(\bar{l}\gamma^\mu l),\\
\mathcal{O}_{10} &= \frac{\alpha_{\text{em}}}{4\pi}(\bar{s}\gamma_\mu P_L b)(\bar{l}\gamma^\mu \gamma_5 l),\\
\mathcal{O}_S &= \frac{\alpha_{\text{em}}}{4\pi}(\bar{s}P_R b)(\bar{l}l),\\
\mathcal{O}_P &= \frac{\alpha_{\text{em}}}{4\pi}(\bar{s}P_R b)(\bar{l}\gamma_5 l),\\
\mathcal{O}_T &= \frac{\alpha_{\text{em}}}{4\pi}(\bar{s}\sigma_{\mu\nu} b)(\bar{l}\sigma^{\mu\nu} l),\\
\mathcal{O}_{7'} &= \frac{e}{16\pi^2} m_b(\bar{s}\sigma_{\mu\nu}P_L b)F^{\mu\nu},\\
\mathcal{O}_{9'} &= \frac{\alpha_{\text{em}}}{4\pi}(\bar{s}\gamma_\mu P_R b)(\bar{l}\gamma^\mu l),\\
\mathcal{O}_{10'} &= \frac{\alpha_{\text{em}}}{4\pi}(\bar{s}\gamma_\mu P_R b)(\bar{l}\gamma^\mu \gamma_5 l),\\
\mathcal{O}_{S'} &= \frac{\alpha_{\text{em}}}{4\pi}(\bar{s}P_L b)(\bar{l}l),\\
\mathcal{O}_{P'} &= \frac{\alpha_{\text{em}}}{4\pi}(\bar{s}P_L b)(\bar{l}\gamma_5 l),\\
\mathcal{O}_{T5} &= \frac{\alpha_{\text{em}}}{4\pi}(\bar{s}\sigma_{\mu\nu} b)(\bar{l}\sigma^{\mu\nu}\gamma_5 l),
\end{aligned}$$

where $P_{L,R} = (1 \mp \gamma_5)/2$ and $m_b \equiv m_b(\mu)$ denotes the running b quark mass in the $\overline{\text{MS}}$ scheme.

Since C_7 and C_9 always appear in particular combinations with other $C_{i\le 6}$ (the operators $\mathcal{O}_{i\le 6}$ are identical to the $P_{i\le 6}$ given in [58,59]) in matrix elements, it is customary to define the following effective Wilson coefficients [58,59]:

$$C_7^{\text{eff}}(\mu) = C_7(\mu) - \frac{1}{3}C_3(\mu) - \frac{4}{9}C_4(\mu) - \frac{20}{3}C_5(\mu) - \frac{80}{9}C_6(\mu)\,, \tag{2.4}$$

$$C_9^{\text{eff}}(\mu) = C_9(\mu) + Y(q^2,\mu)\,, \tag{2.5}$$

where the one loop expression for the function $Y(q^2,\mu)$ can be found in [21,59].

Note that the photonic dipole operators $\mathcal{O}_7$ and $\mathcal{O}_{7'}$ lead to lepton universal contributions modulo lepton mass effects and hence cannot provide an explanation of the R_{K^*} anomalies once bound from $B \to X_s\gamma$ is taken into account [25]. Moreover, as the tensor operators do not get generated at the dimension 6 level if the full SM gauge invariance is imposed [60,61], we ignore them in this work.

3 Results

As the branching ratio of the fully leptonic decay $B_s \to \mu^+\mu^-$ poses strong constraints on some of the Wilson coefficients, we first show the expression of this branching ratio as a function of the relevant couplings [23],

$$\begin{aligned}
\mathcal{B}(B_s \to \mu^+\mu^-) &= \frac{G_F^2\alpha_{em}^2 m_{B_s}^5 f_{B_s}^2 \tau_{B_s}}{64\pi^3}|V_{tb}V_{ts}^*|^2\sqrt{1-\frac{4m_\mu^2}{m_{B_s}^2}}\\
&\times\left\{\left(1-\frac{4m_\mu^2}{m_{B_s}^2}\right)\left|\frac{C_S^\mu - C_{S'}^\mu}{m_b+m_s}\right|^2 + \left|\frac{C_P^\mu - C_{P'}^\mu}{m_b+m_s} + \frac{2m_\mu}{m_{B_s}^2}\right.\right.\\
&\left.\left.\times\,(C_{10}^{\text{SM}} + \Delta C_{10}^\mu - C_{10'}^\mu)\right|^2\right\}.
\end{aligned} \tag{3.1}$$

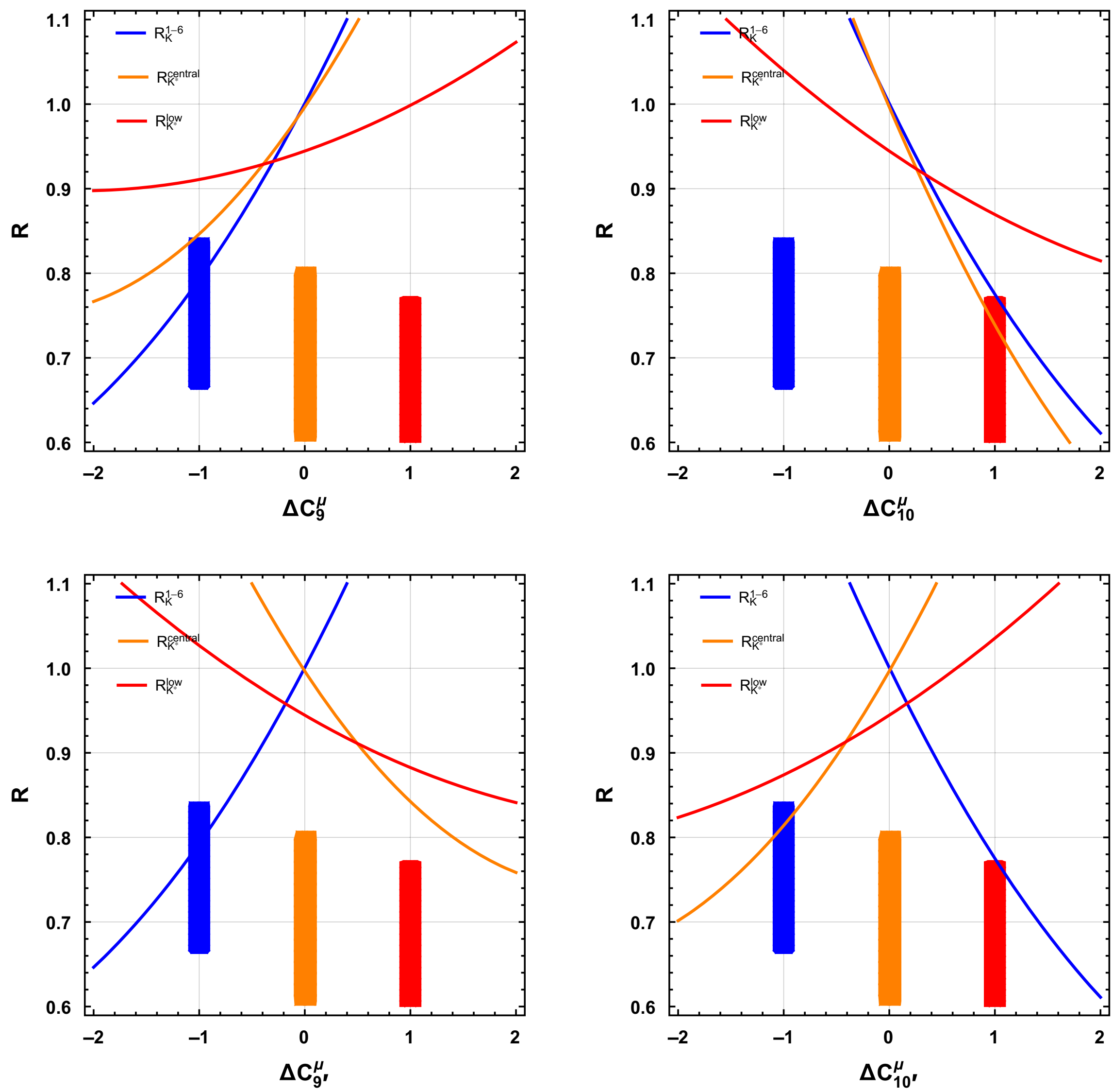

Fig. 4 Variations of R_K, $R_{K^*}^{\rm low}$ and $R_{K^*}^{\rm central}$ with the various vector and axial-vector Wilson coefficients in the muon mode. The vertical bands correspond to the experimental 1σ allowed regions (and independent of ΔC). The legends explain the meaning of the different colors. We only plot the central values of the observables as the uncertainties are expected to be very small in these ratios; see for example [4,13,16]

In Fig. 1, we show how $\mathcal{B}(B_s \to \mu^+\mu^-)$ constraints ΔC_{10}^{μ}, and also the scalar and pseudo scalar operators. The horizontal blue band shows the 1σ experimentally allowed region. Hence, ΔC_{10}^{μ} ($\Delta C_{10'}^{\mu}$) should satisfy $0 \lesssim \Delta C_{10}^{\mu} \lesssim 0.7$ ($-0.7 \lesssim \Delta C_{10'}^{\mu} \lesssim 0$).

Note that, unlike ΔC_{10}^{μ} and $\Delta C_{10'}^{\mu}$, there are practically no bounds on ΔC_{10}^{e} and $\Delta C_{10'}^{e}$ because the experimental upper bound, 2.8×10^{-7} [10], is many orders of magnitude above the SM prediction $(8.35 \pm 0.39) \times 10^{-14}$ [6,7].

The constraints on the scalar operators are extremely severe, as can be seen from the figures.

3.1 One Wilson coefficient at a time

In this section, we consider one Wilson coefficient at a time and investigate whether it can explain all the experimental results within their 1σ values simultaneously. All the numerical results in this section are based on the analytic formulas given in [22,23]. As for the form factors, we use [62] for $B \to K$ matrix elements and [63] for the $B \to K^*$ matrix elements.

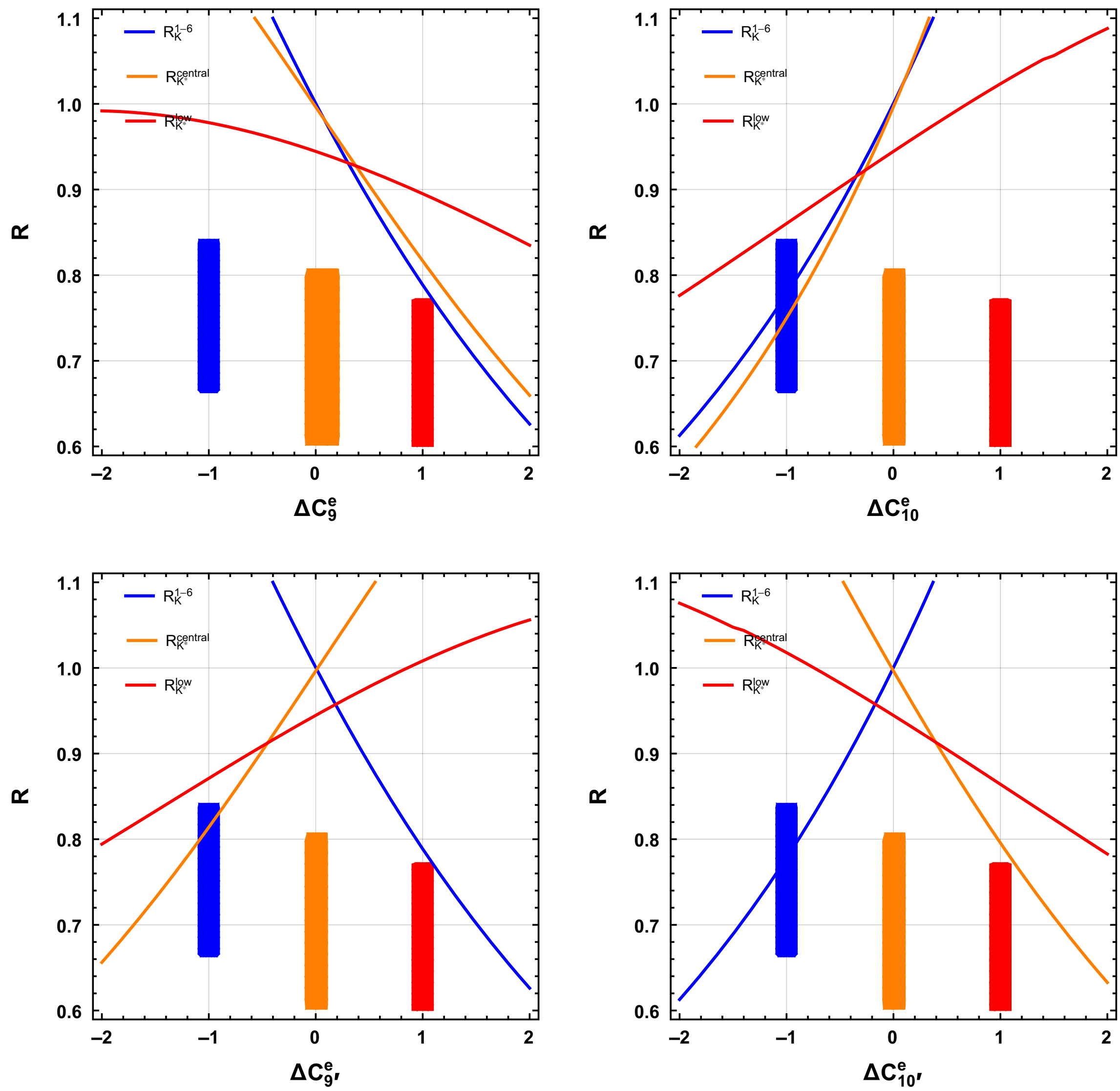

Fig. 5 Variations of R_K, $R_{K^*}^{\rm low}$ and $R_{K^*}^{\rm central}$ with the various vector and axial-vector Wilson coefficients in the electron mode. The vertical bands correspond to the experimental 1σ allowed regions (and independent of ΔC). The legends explain the meaning of the different colors. We only plot the central values of the observables as the uncertainties are expected to be very small in these ratios; see for example [4,13,16]

Scalar and pseudo-scalar operators

We first present our results for the scalar operators. In Fig. 2 we show R_K, $R_{K^*}^{\rm low}$ and $R_{K^*}^{\rm central}$ as functions of the scalar and pseudo-scalar Wilson coefficients C_S, $C_{S'}$, C_P and $C_{P'}$ assuming that they only affect the muon mode. It is clear from the plots that (pseudo) scalar operators involving muons are unable to provide solutions to these anomalies, irrespective of their size.

It can be seen form Fig. 3 that the same statement is also true for the (pseudo) scalar operators involving electrons. However, for the operators involving electrons, solutions to two of the anomalies, R_K and $R_{K^*}^{\rm central}$, are in principle possible. But the upper bound on $\mathcal{B}\left(B_s \to e^+e^-\right)$ (see Table 1) constrains the couplings $C_{S,S',P,P'} \lesssim 1.2$, and rules out the possibility of any such explanations.

Vector and axial-vector operators

We now turn to the vector and axial-vector operators. Figure 4 shows the variations of R_K, $R_{K^*}^{\rm low}$ and $R_{K^*}^{\rm central}$ with respect to the Wilson coefficients C_9^μ, $C_{9'}^\mu$, C_{10}^μ and $C_{10'}^\mu$. It can be seen that even the vector and axial vector operators in the muon mode, when taken one at a time, can not explain all the anomalies within their experimental 1σ regions. Additionally, as mentioned after Eq. 3.1, the axial-vector operators ΔC_{10}^μ and $\Delta C_{10'}^\mu$ are constrained rather strongly by measurement of the branching ratio of $B_s \to \mu^+\mu^-$:

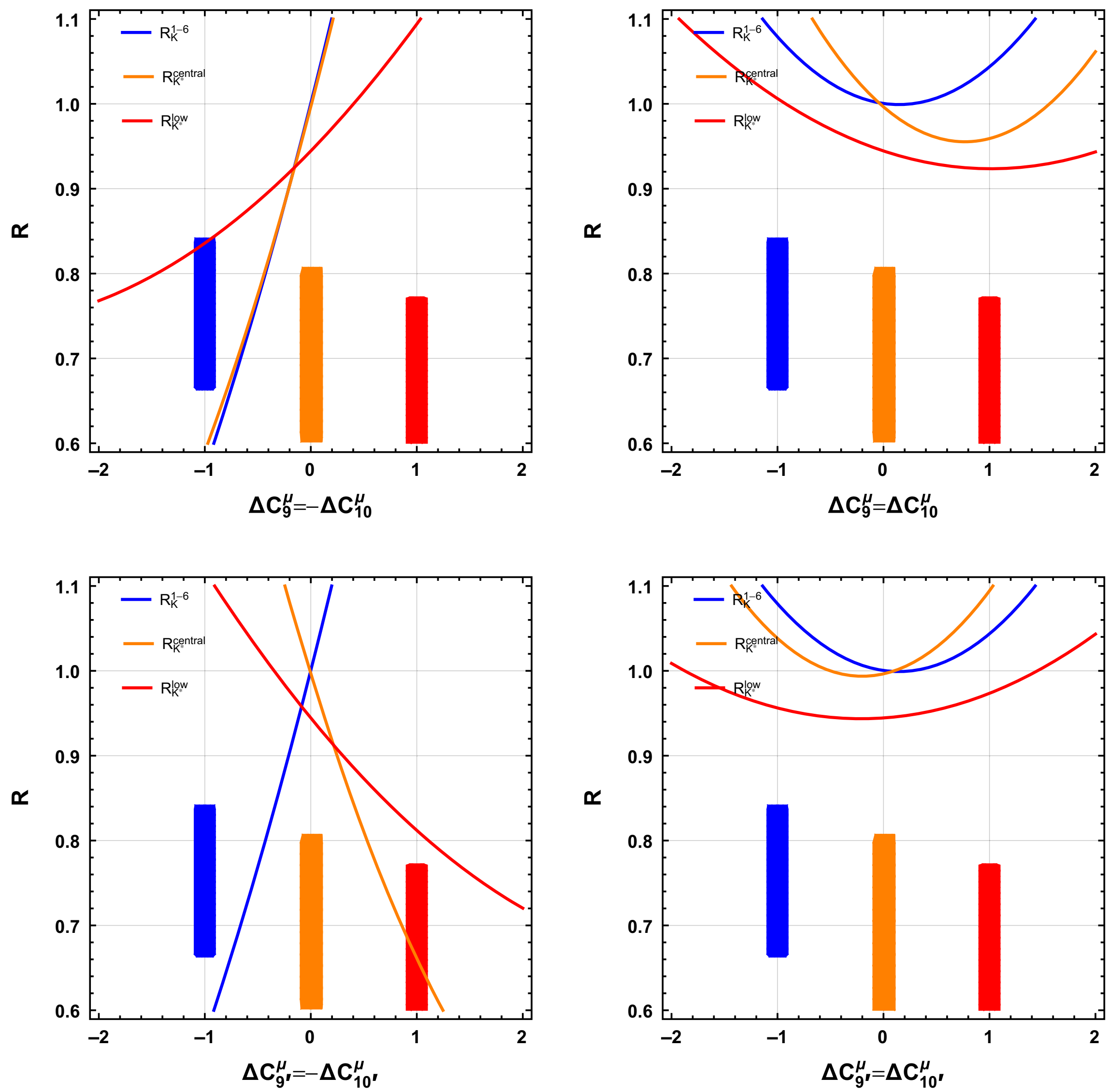

Fig. 6 Variations of R_K, $R_{K^*}^{\rm low}$ and $R_{K^*}^{\rm central}$ with the various vector and axial-vector Wilson coefficients in the muon mode. The vertical bands correspond to the experimental 1σ allowed regions (and independent of ΔC)

$0 \lesssim \Delta C_{10}^\mu \lesssim 0.7$ and $-0.7 \lesssim \Delta C_{10'}^\mu \lesssim 0$. This makes the axial-vector explanation even more unlikely.

Similar statement can also be made about the (axial) vector operators in the electron sector, as can be seen in Fig. 5. However, they do a better job compared to their counterparts in the muon sector. While the primed operators are strongly disfavored, the operator ΔC_{10}^e does comparatively better. For example, $\Delta C_{10}^e = -1.5$ gives $R_K = 0.69$, $R_{K^*}^{\rm central} = 0.66$, $R_{K^*}^{\rm low} = 0.81$, the first two numbers being inside their experimental 1σ regions, and the value of $R_{K^*}^{\rm low}$ is $\sim 1.4\sigma$ away from the experimental central value.

3.2 Combination of Wilson coefficients

In this section, we consider the four cases $\Delta C_{9^{(\prime)}}^\ell = \pm \Delta C_{10^{(\prime)}}^\ell$ for each of $\ell = \mu$ and e. The results are shown in Figs. 6 and 7 for Wilson coefficients involving muons and electrons respectively. The hypotheses $\Delta C_{9^{(\prime)}}^\mu = \Delta C_{10^{(\prime)}}^\mu$ (which correspond to the operators $(\bar{s}\gamma_\alpha P_L b)(\bar{\mu}\gamma^\alpha P_R \mu)$ and $(\bar{s}\gamma_\alpha P_R b)(\bar{\mu}\gamma^\alpha P_R \mu)$) and $\Delta C_{9'}^\mu = -\Delta C_{10'}^\mu$ (which corresponds to the operator $(\bar{s}\gamma_\alpha P_R b)(\bar{\mu}\gamma^\alpha P_L \mu)$) are clearly strongly disfavored.

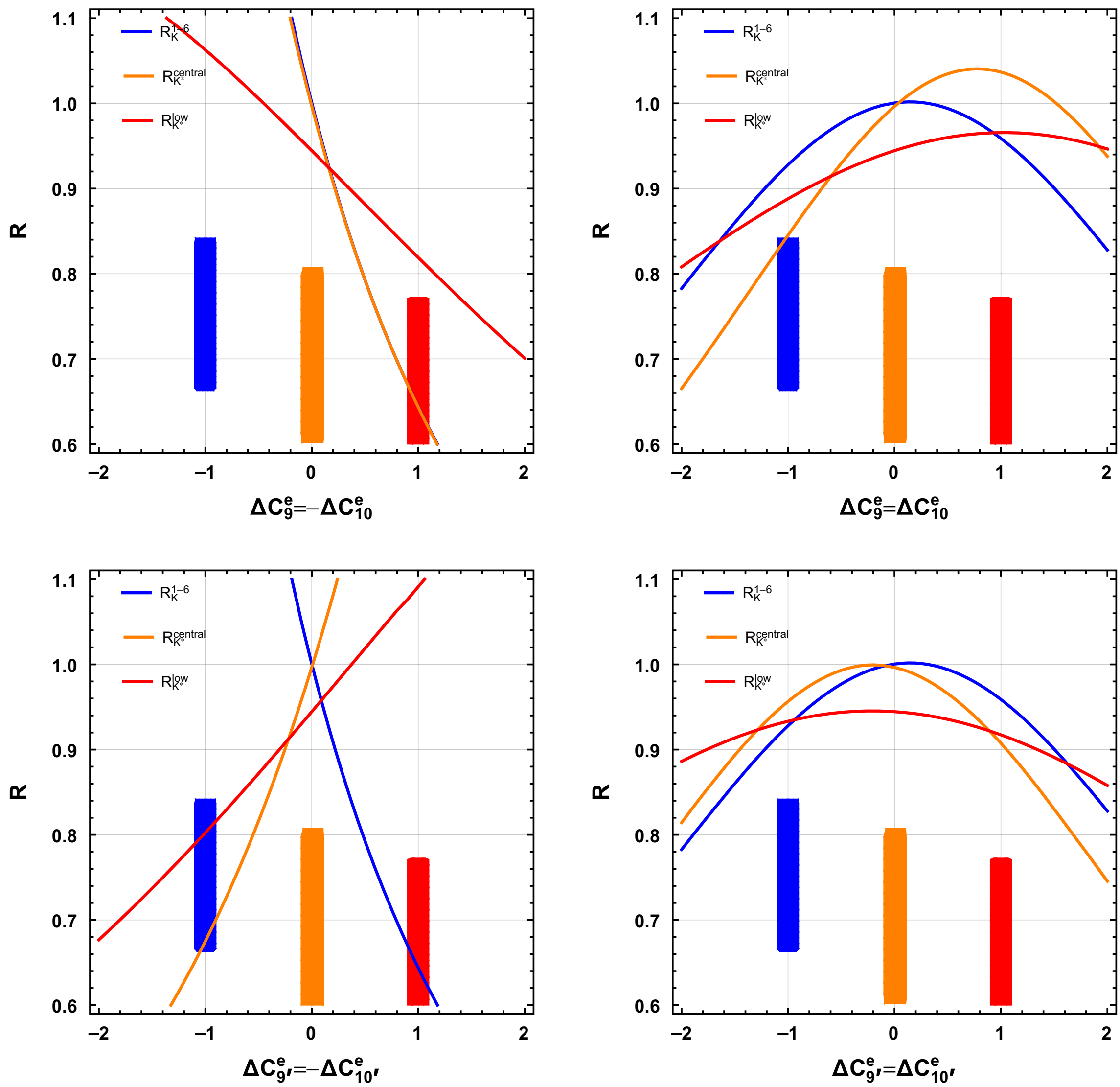

Fig. 7 Variations of R_K, $R_{K^*}^{\text{low}}$ and $R_{K^*}^{\text{central}}$ with the various vector and axial-vector Wilson coefficients in the electron mode. The vertical bands correspond to the experimental 1σ allowed regions (and independent of ΔC)

The other chiral operator $(\bar{s}\gamma_\alpha P_L b)(\bar{\mu}\gamma^\alpha P_L \mu)$ (our hypothesis $\Delta C_9^\mu = -\Delta C_{10}^\mu$) turns out to be the closest to explain all the anomalies. However, even this operator fails to satisfy all the experimental results within their 1σ ranges, in particular the value of $R_{K^*}^{\text{low}}$.

The situation is slightly better for the operators involving electrons. It can be seen from Fig. 7 that, while the primed operators are strongly disfavored, the other two cases: $\Delta C_9^e = -\Delta C_{10}^e \approx 0.8$ and $\Delta C_9^e = \Delta C_{10}^e \approx -2$ work much better. In these two cases, R_K and $R_{K^*}^{\text{central}}$ can be satisfied within 1σ, and $R_{K^*}^{\text{low}}$ within $\sim 1.5\sigma$ and $\sim 1.3\sigma$, respectively.

The scenarios $\Delta C_9^{e,\mu} = \pm\Delta C_{9'}^{e,\mu}$ and $\Delta C_{10}^{e,\mu} = \pm\Delta C_{10'}^{e,\mu}$ are shown in Figs. 8 and 9. It can be seen that they do not do a good job in explaining the anomalies simultaneously.

Before closing this section, we would like to mention that we have also explored the possibility of existence of a pair of NP operators simultaneously with unrelated Wilson coefficients. For example, we have tried the following combinations: $(\Delta C_9^\mu, \Delta C_9^e)$, $(\Delta C_{10}^\mu, \Delta C_{10}^e)$, $(\Delta C_9^\mu = -\Delta C_{10}^\mu, \Delta C_9^e = -\Delta C_{10}^e)$, $(\Delta C_9^\mu = \Delta C_{10}^\mu, \Delta C_9^e = \Delta C_{10}^e)$ and all the 6 possible combinations $(\Delta C_X^\mu, \Delta C_Y^\mu)$ $(X, Y = 9, 10, 9', 10')$. However, even in these cases, we have not found solutions that explain R_K, $R_{K^*}^{\text{central}}$ and $R_{K^*}^{\text{low}}$ simultaneously within their respective 1σ allowed regions.

Hence, we conclude that, while local 4-Fermi operators of certain Lorentz structures (for example, $\Delta C_9^e = -\Delta C_{10}^e \approx 0.8$ as advertised above) can definitely reduce the tension with the SM considerably, they fail to bring all the three ratios within their experimental 1σ regions, in particular R_{K^*} in the bin $q^2 = [0.045\text{–}1.1]$ GeV^2.

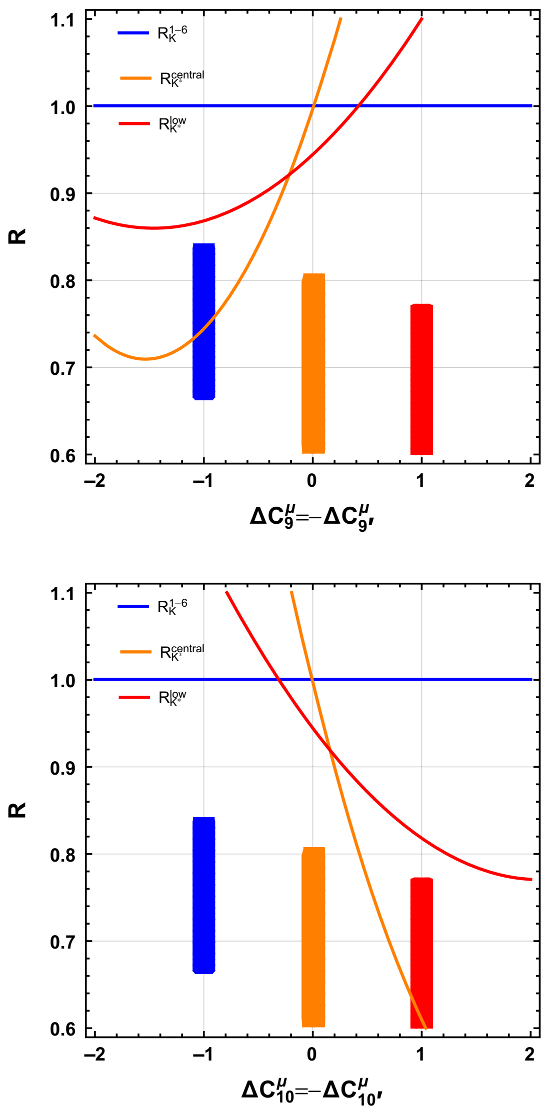

Fig. 8 Variations of R_K, $R_{K^*}^{\rm low}$ and $R_{K^*}^{\rm central}$ with the various vector and axial-vector Wilson coefficients in the muon mode. The vertical bands correspond to the experimental 1σ allowed regions (and independent of ΔC)

3.3 Light vector boson to explain R_{K^*} in the bin $q^2 = [0.045–1.1]$ GeV^2

Our investigations above show that local new physics (i.e., q^2 independent Wilson coefficients) is unable to simultaneously explain R_K, $R_{K^*}^{\rm central}$ and $R_{K^*}^{\rm low}$ at the 1σ level. The main obstacle is to explain the result of R_{K^*} in the low bin. This can be understood by noting that the branching ratio in the low q^2 region is dominated by the Wilson coefficient C_7 which is always lepton flavor universal. Quantitatively, in the q^2 bin [0.045–1.1] GeV^2, the pure C_7 contribution constitutes approximately 73% of the total branching ratio in the SM. On the other hand, the pure C_7 contribution is just about 16% for the q^2 bin [1.1–6] GeV^2.

However, the situation can change in the presence of light degrees of freedom, for example, a very light ($\lesssim$ 20 MeV) vector boson A'_μ, with couplings

$$\mathcal{L} \supset -(\kappa_{bs}\, \bar{b}\gamma_\mu P_L s\, A'_\mu + \text{h.c.}) - \kappa_{ee}\, \bar{e}\gamma_\mu P_L e\, A'_\mu\,. \quad (3.2)$$

The tree level exchange of the vector boson A'_μ generates 'q^2 dependent Wilson coefficients',

$$\Delta C_9^e = -\Delta C_{10}^e = -\frac{1}{2}\left[\frac{4G_F}{\sqrt{2}}\frac{\alpha_{\rm em}}{4\pi}|V_{tb}V_{ts}^*|\right]^{-1}\frac{\kappa_{bs}\kappa_{ee}}{(q^2-m_{A'}^2)} \quad (3.3)$$

$$= -(6.15\times 10^8)\frac{\kappa_{bs}\kappa_{ee}}{(q^2-m_{A'}^2)\,[\text{in GeV}^2]}\,. \quad (3.4)$$

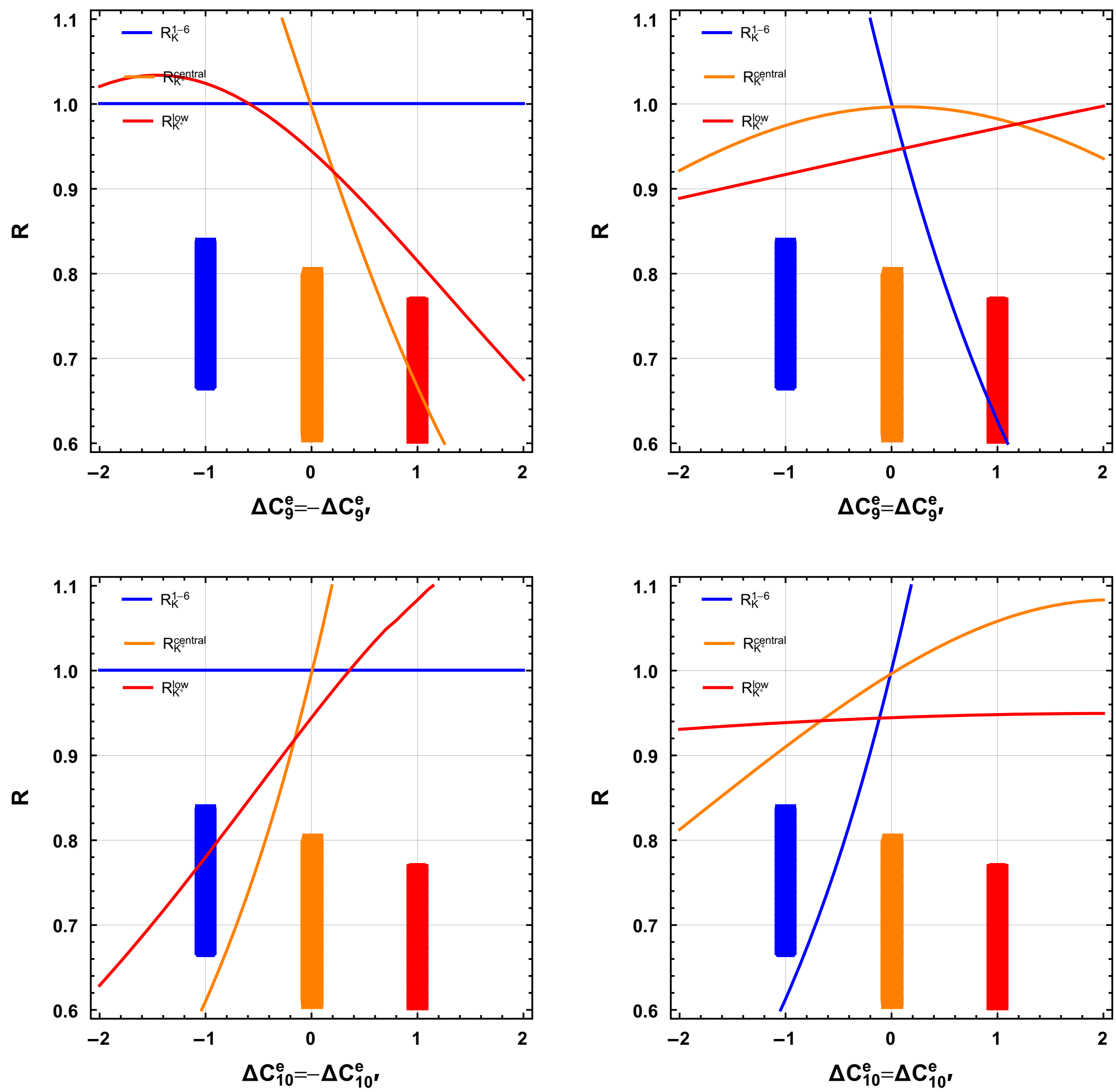

Fig. 9 Variations of R_K, $R_{K^*}^{\rm low}$ and $R_{K^*}^{\rm central}$ with the various vector and axial-vector Wilson coefficients in the muon mode. The vertical bands correspond to the experimental 1σ allowed regions (and independent of ΔC)

The coupling combination $\kappa_{bs}\kappa_{ee} = -0.8 \times 10^{-9}$ generates $R_{K^*}^{\rm low}$ close to its experimental central value.[2] In Fig. 10, we show how $R_{K^*}^{\rm low}$ varies with $\kappa_{bs}\kappa_{ee}$. It can be seen that $-1.1 \times 10^{-9} \lesssim \kappa_{bs}\kappa_{ee} \lesssim -0.5 \times 10^{-9}$ is consistent with the experimental 1σ range of $R_{K^*}^{\rm low}$. We have also checked that values of $\kappa_{bs}\kappa_{ee}$ in the above range can easily be made consistent with the constraints coming from $\bar{B}_s$–B_s mixing and anomalous magnetic moment of electron.

However, the range $-1.1\times10^{-9} \lesssim \kappa_{bs}\kappa_{ee} \lesssim -0.5\times10^{-9}$ generates R_K and $R_{K^*}^{\rm central}$ in the range $0.89 \lesssim R_K, R_{K^*}^{\rm central} \lesssim 0.95$, well outside the experimental 1σ regions. Thus, separate local NP contributions, as discussed in the previous sections, are needed to explain R_K and $R_{K^*}^{\rm central}$.

We have checked that instead of a completely left-chiral coupling in Eq. 3.2, one can also use the following scenario:

$$\mathcal{L} \supset -(\bar{b}\gamma_\mu(\kappa_{bs}^L P_L + \kappa_{bs}^R P_R)s\, A'_\mu + \text{h.c.}) - \kappa_{ee}^V \bar{e}\gamma_\mu e\, A'_\mu, \tag{3.5}$$

which generates both ΔC_9^e and $\Delta C_{9'}^e$ and works better than the previous case. For example, $(\kappa_{bs}^L\kappa_{ee}^V \approx -3.4 \times 10^{-9}$, $\kappa_{bs}^R\kappa_{ee}^V \approx -1.8 \times 10^{-9})$ produces $R_{K^*}^{\rm low} \approx 0.67$, $R_{K^*}^{\rm central} \approx 0.93$, $R_K \approx 0.75$.

4 Summary

In this paper, we have performed a model independent analysis of the recent LHCb measurements of R_{K^*} in the two dilepton invariant mass bins $q^2 \equiv m_{\ell\ell}^2 = [0.045–1.1]\ \text{GeV}^2$

[2] We find that a light gauge boson that couples to muons, instead of electrons, is unable to reproduce $R_{K^*}^{\rm low}$ below 0.8.

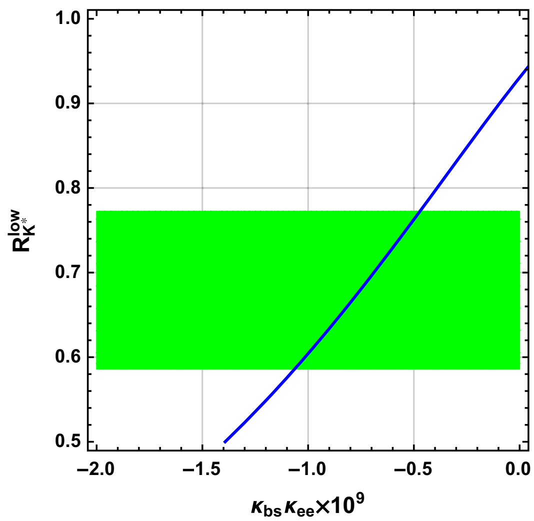

Fig. 10 Variations of $R_{K^*}^{\rm low}$ with $\kappa_{bs}\kappa_{ee}$. The green band corresponds to the experimental 1σ allowed region. We have used $m_{A'} = 17$ MeV in the numerical calculations. However, the result is not sensitive to the exact value of $m_{A'}$ as long as it is $\lesssim$ 50 MeV

and [1.1–6] GeV^2, along with an older measurement of a similar ratio R_K in the pseudo-scalar meson mode. We consider various possible $[\bar{b}\Gamma_\mu s][\bar{\ell}\Gamma^\mu \ell]$ operator structures (both for the muon and electron modes), switching one operator at a time and also for specific combinations of them. We show that all the NP (pseudo-) scalar operators and most of the (axial) vector operators are strongly disfavored by the data. While some (axial-) vector operators can explain R_K and $R_{K^*}^{\rm central}$ at the same time, we found no operator that can explain all the three ratios (in particular, $R_{K^*}^{\rm low}$) simultaneously within their 1σ experimental ranges.

In order to explain also the $R_{K^*}^{\rm low}$, we proposed the existence of a very light ($\lesssim$ 20 MeV) vector boson with flavor specific couplings. We gave two examples shown in Eqs. 3.2 and 3.5. In the first case, we find that this new gauge boson, with couplings that explain $R_{K^*}^{\rm low}$, can neither explain R_K or $R_{K^*}^{\rm central}$. Thus, additional local operators will be required to explain them together. As an example, a light gauge boson with coupling

$$\kappa_{bs}\kappa_{ee} = -0.6 \times 10^{-9} \qquad (4.1)$$

and additional local NP Wilson coefficients $\Delta C_9^\mu = -\Delta C_{10}^\mu = -0.6$ generates

$$R_K = 0.69\,,\ R_{K^*}^{\rm central} = 0.69 \text{ and } R_{K^*}^{\rm low} = 0.65\,, \qquad (4.2)$$

all close to their experimental central values.

In the second case, both $R_{K^*}^{\rm low}$ and R_K could be explained by the light vector only, however, an explanation of $R_{K^*}^{\rm central}$ as well would require additional, perhaps short distance, new physics.

It remains a challenge to connect the existence of the light vector boson (with specific couplings) to heavy NP that generates the required short distance Wilson coefficients. We leave that for future work.

We close with the comment that there might be issues with both the theoretical SM prediction (in particular, the uncertainty due to QED corrections) and the experimental measurement of R_{K^*} in the low bin. In this work, we have taken the most recent SM prediction, the associated theoretical uncertainty and the experimental measurement at face value. Needless to mention that our conclusions may change if either of SM prediction/uncertainty or the experimental measurement changes in the future.

Acknowledgements We thank Daniel Aloni for many useful discussions, comments on the manuscript and help with numerical calculations. Fruitful discussions with Ryosuke Sato, Masahiro Takimoto and Gilad Perez are also gratefully acknowledged. We also acknowledge the public code flavio [64] which has been used to cross-check some of the numerical results.

References

1. S. Descotes-Genon, L. Hofer, J. Matias, J. Virto, Global analysis of $b \to s\ell\ell$ anomalies. JHEP **06**, 092 (2016). arXiv:1510.04239
2. M. Bordone, G. Isidori, A. Pattori, On the standard model predictions for R_K and R_{K^*}. Eur. Phys. J. C **76**, 440 (2016). arXiv:1605.07633
3. LHCb collaboration collaboration, R. Aaij et al., Test of lepton universality using $B^+ \to K^+\ell^+\ell^-$ decays. arXiv:1406.6482
4. B. Capdevila, A. Crivellin, S. Descotes-Genon, J. Matias, J. Virto, Patterns of new physics in $b \to s\ell^+\ell^-$ transitions in the light of recent data. arXiv:1704.05340
5. S. Bifani, Talk for the LHCb collaboration, CERN, 18/4/2016. https://indico.cern.ch/event/580620/
6. C. Bobeth, M. Gorbahn, T. Hermann, M. Misiak, E. Stamou et al., $B_{s,d} \to l^+l^-$ in the standard model with reduced theoretical uncertainty. Phys. Rev. Lett. **112**, 101801 (2014). arXiv:1311.0903
7. R. Fleischer, R. Jaarsma, G. Tetlalmatzi-Xolocotzi, In pursuit of new physics with $B^0_{s,d} \to \ell^+\ell^-$. arXiv:1703.10160
8. CMS collaboration, S. Chatrchyan et al., Measurement of the B(s) to mu+ mu− branching fraction and search for B0 to mu+ mu− with the CMS experiment. Phys. Rev. Lett. **111**, 101804 (2013). arXiv:1307.5025
9. LHCb collaboration, R. Aaij et al., Measurement of the $B_s^0 \to \mu^+\mu^-$ branching fraction and effective lifetime and search for $B^0 \to \mu^+\mu^-$ decays. arXiv:1703.05747
10. CDF collaboration, T. Aaltonen et al., Search for the decays $B_s^0 \to e^+\mu^-$ and $B_s^0 \to e^+e^-$ in CDF Run II. Phys. Rev. Lett. **102**, 201801 (2009). arXiv:0901.3803
11. D. Bardhan, P. Byakti, D. Ghosh, A closer look at the R_D and R_{D^*} anomalies. JHEP **01**, 125 (2017). arXiv:1610.03038

12. R. Alonso, B. Grinstein, J. Martin Camalich, The lifetime of the B_c^- meson and the anomalies in $B \to D^{(*)}\tau\nu$. Phys. Rev. Lett. **118**, 081802 (2017). arXiv:1611.06676
13. W. Altmannshofer, P. Stangl, D.M. Straub, Interpreting hints for lepton flavor universality violation. arXiv:1704.05435
14. G. D'Amico, M. Nardecchia, P. Panci, F. Sannino, A. Strumia, R. Torre et al., Flavour anomalies after the R_{K^*} measurement. arXiv:1704.05438
15. G. Hiller, I. Nisandzic, R_K and R_{K^*} beyond the standard model. arXiv:1704.05444
16. L.-S. Geng, B. Grinstein, S. Jager, J. Martin Camalich, X.-L. Ren, R.-X. Shi, Towards the discovery of new physics with lepton-universality ratios of $b \to s\ell\ell$ decays. arXiv:1704.05446
17. M. Ciuchini, A.M. Coutinho, M. Fedele, E. Franco, A. Paul, L. Silvestrini et al., On Flavourful Easter eggs for new physics hunger and lepton flavour universality violation. arXiv:1704.05447
18. A. Celis, J. Fuentes-Martin, A. Vicente, J. Virto, Gauge-invariant implications of the LHCb measurements on lepton-flavour non-universality. arXiv:1704.05672
19. D. Becirevic, O. Sumensari, A leptoquark model to accommodate $R_K^{\rm exp} < R_K^{\rm SM}$ and $R_{K^*}^{\rm exp} < R_{K^*}^{\rm SM}$. arXiv:1704.05835
20. G. Hiller, F. Kruger, More model independent analysis of $b \to s$ processes. Phys. Rev. D **69**, 074020 (2004). arXiv:hep-ph/0310219
21. W. Altmannshofer, P. Ball, A. Bharucha, A.J. Buras, D.M. Straub et al., Symmetries and asymmetries of $B \to K^*\mu^+\mu^-$ decays in the standard model and beyond. JHEP **0901**, 019 (2009). arXiv:0811.1214
22. A.K. Alok, A. Dighe, D. Ghosh, D. London, J. Matias et al., New-physics contributions to the forward–backward asymmetry in $B \to K^*\mu^+\mu^-$. JHEP **1002**, 053 (2010). arXiv:0912.1382
23. A.K. Alok, A. Datta, A. Dighe, M. Duraisamy, D. Ghosh et al., New physics in $b \to s\mu^+\mu^-$: CP-conserving observables. JHEP **1111**, 121 (2011). arXiv:1008.2367
24. A.K. Alok, A. Datta, A. Dighe, M. Duraisamy, D. Ghosh et al., New physics in $b \to s\mu + \mu-$: CP-violating observables. JHEP **1111**, 122 (2011). arXiv:1103.5344
25. S. Descotes-Genon, D. Ghosh, J. Matias, M. Ramon, Exploring new physics in the C7–C7' plane. JHEP **1106**, 099 (2011). arXiv:1104.3342
26. W. Altmannshofer, P. Paradisi, D.M. Straub, Model-independent constraints on new physics in $b \to s$ transitions. JHEP **1204**, 008 (2012). arXiv:1111.1257
27. J. Matias, F. Mescia, M. Ramon, J. Virto, Complete anatomy of $\bar{B}_d \to \bar{K}^{*0}(\to K\pi)l^+l^-$ and its angular distribution. JHEP **1204**, 104 (2012). arXiv:1202.4266
28. S. Descotes-Genon, J. Matias, M. Ramon, J. Virto, Implications from clean observables for the binned analysis of $B \to K*\mu^+\mu^-$ at large recoil. JHEP **1301**, 048 (2013). arXiv:1207.2753
29. J. Lyon, R. Zwicky, Isospin asymmetries in $B \to (K^*, \rho)\gamma/l^+l^-$ and $B \to Kl^+l^-$ in and beyond the standard model. arXiv:1305.4797
30. S. Descotes-Genon, J. Matias, J. Virto, Understanding the $B \to K^*\mu^+\mu^-$ anomaly. Phys. Rev. D **88**, 074002 (2013). arXiv:1307.5683
31. W. Altmannshofer, D.M. Straub, New physics in $B \to K^*\mu\mu$? Eur. Phys. J. C **73**, 2646 (2013). arXiv:1308.1501
32. A.J. Buras, J. Girrbach, Left-handed Z' and Z FCNC quark couplings facing new $b \to s\mu^+\mu^-$ data. JHEP **1312**, 009 (2013). arXiv:1309.2466
33. A. Datta, M. Duraisamy, D. Ghosh, Explaining the $B \to K^*\mu^+\mu^-$ data with scalar interactions. Phys. Rev. D **89**, 071501 (2014). arXiv:1310.1937
34. D. Ghosh, M. Nardecchia, S.A. Renner, Hint of lepton flavour non-universality in B meson decays. JHEP **12**, 131 (2014). arXiv:1408.4097
35. F.S. Queiroz, K. Sinha, A. Strumia, Leptoquarks, dark matter, and anomalous LHC events. Phys. Rev. D **91**, 035006 (2015). arXiv:1409.6301
36. R. Mandal, R. Sinha, D. Das, Testing new physics effects in $B \to K^*\ell^+\ell^-$. Phys. Rev. D **90**, 096006 (2014). arXiv:1409.3088
37. A. Greljo, G. Isidori, D. Marzocca, On the breaking of lepton flavor universality in B decays. JHEP **07**, 142 (2015). arXiv:1506.01705
38. B. Gripaios, M. Nardecchia, S.A. Renner, Linear flavour violation and anomalies in B physics. JHEP **06**, 083 (2016). arXiv:1509.05020
39. R. Barbieri, G. Isidori, A. Pattori, F. Senia, Anomalies in B-decays and $U(2)$ flavour symmetry. Eur. Phys. J. C **76**, 67 (2016). arXiv:1512.01560
40. S. Sahoo, R. Mohanta, Scalar leptoquarks and the rare B meson decays. Phys. Rev. D **91**, 094019 (2015). arXiv:1501.05193
41. S. Sahoo, R. Mohanta, A.K. Giri, Explaining the R_K and $R_{D^{(*)}}$ anomalies with vector leptoquarks. Phys. Rev. D **95**, 035027 (2017). arXiv:1609.04367
42. F. Feruglio, P. Paradisi, A. Pattori, Revisiting lepton flavor universality in B decays. Phys. Rev. Lett. **118**, 011801 (2017). arXiv:1606.00524
43. R. Barbieri, C.W. Murphy, F. Senia, B-decay anomalies in a composite leptoquark model. Eur. Phys. J. C **77**, 8 (2017). arXiv:1611.04930
44. I. Garcia Garcia, LHCb anomalies from a natural perspective. JHEP **03**, 040 (2017). arXiv:1611.03507
45. E. Megias, G. Panico, O. Pujolas, M. Quiros, A natural origin for the LHCb anomalies. JHEP **09**, 118 (2016). arXiv:1608.02362
46. B. Bhattacharya, A. Datta, J.-P. Guevin, D. London, R. Watanabe, Simultaneous explanation of the R_K and $R_{D^{(*)}}$ puzzles: a model analysis. JHEP **01**, 015 (2017). arXiv:1609.09078
47. D. Bhatia, S. Chakraborty, A. Dighe, Neutrino mixing and R_K anomaly in $U(1)_X$ models: a bottom-up approach. JHEP **03**, 117 (2017). arXiv:1701.05825
48. E. Megias, M. Quiros, L. Salas, Lepton-flavor universality violation in $R_{D^{(*)}}$ and R_K from warped space. arXiv:1703.06019
49. A. Datta, J. Liao, D. Marfatia, A light Z' for the R_K puzzle and nonstandard neutrino interactions. Phys. Lett. B **768**, 265–269 (2017). arXiv:1702.01099
50. P. Ball, G.W. Jones, R. Zwicky, $B \to V\gamma$ beyond QCD factorisation. Phys. Rev. D **75**, 054004 (2007). arXiv:hep-ph/0612081
51. A. Khodjamirian, T. Mannel, A. Pivovarov, Y.-M. Wang, Charm-loop effect in $B \to K^{(*)}\ell^+\ell^-$ and $B \to K^*\gamma$. JHEP **1009**, 089 (2010). arXiv:1006.4945
52. M. Dimou, J. Lyon, R. Zwicky, Exclusive chromomagnetism in heavy-to-light FCNCs. Phys. Rev. D **87**, 074008 (2013). arXiv:1212.2242
53. S. Jager, J. Martin Camalich, On $B \to V\ell\ell$ at small dilepton invariant mass, power corrections, and new physics. JHEP **05**, 043 (2013). arXiv:1212.2263
54. J. Lyon, R. Zwicky, Resonances gone topsy turvy—the charm of QCD or new physics in $b \to s\ell^+\ell^-$? arXiv:1406.0566
55. M. Ciuchini, M. Fedele, E. Franco, S. Mishima, A. Paul, L. Silvestrini et al., $B \to K^*\ell^+\ell^-$ decays at large recoil in the standard model: a theoretical reappraisal. JHEP **06**, 116 (2016). arXiv:1512.07157
56. S. Jager, J.M. Camalich, Reassessing the discovery potential of the $B \to K^*\ell^+\ell^-$ decays in the large-recoil region: SM challenges and BSM opportunities. Phys. Rev. D **93**, 014028 (2016). arXiv:1412.3183
57. B. Capdevila, S. Descotes-Genon, L. Hofer, J. Matias, Hadronic uncertainties in $B \to K^*\mu^+\mu^-$: a state-of-the-art analysis. JHEP **04**, 016 (2017). arXiv:1701.08672
58. K.G. Chetyrkin, M. Misiak, M. Munz, Weak radiative B meson decay beyond leading logarithms. Phys. Lett. B **400**, 206–219 (1997). arXiv:hep-ph/9612313

59. C. Bobeth, M. Misiak, J. Urban, Photonic penguins at two loops and m_t dependence of $BR[B \to X_s l^+ l^-]$. Nucl. Phys. B **574**, 291–330 (2000). arXiv:hep-ph/9910220
60. B. Grzadkowski, M. Iskrzynski, M. Misiak, J. Rosiek, Dimension-six terms in the standard model Lagrangian. JHEP **10**, 085 (2010). arXiv:1008.4884
61. R. Alonso, B. Grinstein, J. Martin Camalich, $SU(2) \times U(1)$ gauge invariance and the shape of new physics in rare B decays. Phys. Rev. Lett. **113**, 241802 (2014). arXiv:1407.7044
62. HPQCD collaboration, C. Bouchard, G.P. Lepage, C. Monahan, H. Na, J. Shigemitsu, Rare decay $B \to K\ell^+\ell^-$ form factors from lattice QCD. Phys. Rev. D **88**, 054509 (2013). arXiv:1306.2384
63. A. Bharucha, D.M. Straub, R. Zwicky, $B \to V\ell^+\ell^-$ in the standard model from light-cone sum rules. JHEP **08**, 098 (2016). arXiv:1503.05534
64. D. Straub, P. Stangl, C. Niehoff, E. Gurler, J. Kumar, Sreicher et al., flav-io/flavio v0.21 (2017). doi:10.5281/zenodo.555949